Photodiagnosis and Photodynamic Therapy 27 (2019) 268–275

Contents lists available at ScienceDirect

Photodiagnosis and Photodynamic Therapy

journal homepage: www.elsevier.com/locate/pdpdt

In vitro photodynamic therapy of endothelial cells using hematoporphyrin monomethyl ether (Hemoporfin): Relevance to treatment of port wine stains

Yingjuan Mei[a], Xiangling Xiao[a,b], Lili Fan[a], Qichao Liu[a,b], Mengxue Zheng[a], Michael R. Hamblin[c,d,e], Bing Ni[f], Rui Yin[a,*]

[a] Department of Dermatology, Southwest Hospital, Third Military Medical University (Army Medical University), Chongqing 400038, China
[b] State Key Laboratory of Silkworm Genome Biology, Southwest University, Chongqing, 400715, China
[c] Wellman Center for Photomedicine, Massachusetts General Hospital, Boston, MA, 02114, USA
[d] Department of Dermatology, Harvard Medical School, Boston, MA, 02115, USA
[e] Harvard-MIT Division of Health Sciences and Technology, Cambridge, MA 02139, USA
[f] Department of Pathophysiology, Third Military Medical University (Army Medical University), Chongqing 400038, China

ARTICLE INFO

Keywords:
Port wine stains
Photodynamic therapy
Endothelial cells
Hemoporfin
Apoptosis
Signaling pathway
Vascular endothelial growth factor
VEGF/Akt/mTOR pathway

ABSTRACT

Hemoporfin (hematoporphyrin monomethyl ether, HMME) is a relatively new photosensitizer that has achieved success in mediating photodynamic therapy (PDT) of port wine stains in China. However, the exact mechanism of Hemoporfin PDT on endothelial cell proliferation and apoptosis is unclear. The present study investigated the mechanism of action of HMME-PDT on endothelial cells in vitro. Human umbilical vein endothelial cells (HUVECs) were cultured in vitro. HMME-PDT treated the cells and detected the phototoxicity by cell counting kit-8 (CCK-8) assay, apoptosis by Flow cytometry assay and quantification of the secreted VEGF-A levels using ELISA and different proteins expression by quantitative real-time PCR and Western blotting. Phototoxicity was caused in an HMME and light dose-dependent manner. Apoptosis was induced as shown by Annexin-V/propidium iodide staining and morphological changes. The Bax/Bcl-2 ratio was increased as shown by Western blot for protein and RT-qPCR for mRNA. VEGF-A expression was reduced and signaling molecules in the Akt/mTOR pathway were inhibited as shown by ELISA and immunofluorescence. Hemoporfin (hematoporphyrin monomethyl ether, HMME) has achieved success in mediating photodynamic therapy (PDT) of port wine stains. The clinical success of HMME-PDT with low recurrence rates can be explained by inhibition of endothelial cell proliferation through VEGF/Akt /mTOR pathway.

1. Introduction

Port wine stains, also known as *nevus flammeus* or *nevus telangiectaticus*, are the congenital superficial capillary hyperplasia. The incidence of port wine stains is generally 0.3% to 0.5% in the population [1]. Port wine stains usually do not spontaneously resolve [2]. The skin lesions mainly appear as pink-to-red macules or patches in the early stage, and grow proportionally with age and often progressively darken to deep red or purple and gradually thicken [3]. About 65% of the patients have nodules in adulthood and some patients are prone to spontaneous bleeding [2,3]. The disease mainly occurs in exposed bodily parts such as the face and neck, seriously affecting the patient's appearance, resulting in a decline in the quality of life of the patient and an increase in mental stress [4,5]. Based on the principle of selective photothermal action, the pulsed dye laser (PDL) has become the gold standard for the treatment of port wine stains [6]. Most of the patients can obtain 50–75% improvement after multiple sessions of treatment [7]. Nevertheless, the rate of complete resolution of the lesions is still less than 25%, and a large number of PWS patients may develop resistance to PDL after a prolonged period of treatment [7].

New therapeutic approaches that overcome the limitations of traditional treatments are needed. The best approach is to increase the damage to endothelial cells with the minimal damage to the adjacent normal cells for reducing the recurrence rate. Photodynamic therapy (PDT) provides an alternative method of treating diseases due to unwanted tissue, which is based on the generation of reactive oxygen species (ROS) by light-activated photosensitizers or non-toxic dyes [8,9]. The ROS is generated by the interaction between oxygen, photosensitizer, and light PDT [10]. The ROS modulate various aspects destruction of tissues and cells by inducing oxidative stress for blood

* Corresponding author.
E-mail address: swyinrui@163.com (R. Yin).

https://doi.org/10.1016/j.pdpdt.2019.06.003
Received 13 March 2019; Received in revised form 1 May 2019; Accepted 7 June 2019
Available online 08 June 2019
1572-1000/

vessels and surrounding immune response. Therefore, the quantity and location of the ROS generation influences the potency of PDT [11]. Hemoporfin, also called [7(12)-(1-methoxyethyl)-12(7)-(1-hydroxyethyl)-3,8,13,17-tetramethyl-21H,23H-porphin-2,18-dipropionic acid], or hematoporphyrin monomethyl ether (HMME), is a porphyrin derivative widely studied in China [12]. Compared with first generation PDT drugs such as hematoporphyrin derivative, Hemoporfin has a stable structure, stronger photodynamic efficiency, higher photoactivity, faster clearance rate and lower toxicity [12,13].

PDT-induced cell death is primarily caused by apoptosis, necrosisand autophagy, in which apoptosis is the most key processes [14–16]. Several stimuli are known to trigger apoptosis, which is a programmed cell death process. Some of these stimuli include oxidative stress, which is caused by photosensitization [17] In vivo and in vitro experiments have shown that apoptosis is a major event in the early response to PDT [18]. Hemoporfin photodynamic therapy (HMME-PDT) is a new approach for PWS treatment, in which a photosensitizer localizes within the malformed vascular endothelium and light-activation kills the abnormal cells [19]. However, the exact mechanism of Hemoporfin PDT is unclear, and to our knowledge there has been no study on its effects on endothelial cell proliferation and apoptosis. Therefore, endothelial cells proliferation and apoptosis after HMME-PDT were assessed to determine the effect of PDT at the cellular level in this study.

2. Materials and methods

2.1. Photosensitizer

Hemoporfin[7(12)-(1-methoxyethyl)-12(7)-(1-hydroxyethyl)-3,8,13,17-tetramethyl-21H,23H-porphin-2,18-dipropionic acid](HMME) was provided by Fudan Zhangjiang Bio-Pharmaceutical Co., Ltd., Shanghai, China. A stock solution of Hemoporfin (10 mg/ml) was made in 0.9% NaCl and kept in the dark at −20 °C for no longer than one month. The working solution of Hemoporfin was diluted in high-glucose Dulbecco's Modified Eagle Medium (DMEM, Gibco, USA) medium without fetal calf serum (FCS).

2.2. Cell lines and cell culture

Human umbilical vein endothelial cells (HUVECs) were bought from American Type Culture Collection (ATCC®, PCS-100-010™). The cells were maintained in high-glucose DMEM (Gibco, USA) in the presence of 100 μg/ml streptomycin at 37 °C, 100 U/ml penicillin, and 10% fetal bovine serum (FBS, Biological Industries,USA), in a humidified incubator with 5% CO_2.

2.3. Photodynamic treatment

HUVECs were seeded on culture plates and then subjected to PDT. After 24 h culture, the supernatants were removed, cells were washed using phosphate-buffered saline (PBS) twice and then added the working solution of Hemoporfin for 1 h incubation in darkness. The medium was replaced with PBS, followed by irradiation by a 532-nm LED light (LED-IE-PDT; Wuhan Yage Optic and Electronic Technique Co., Ltd, Wuhan, China) [12,13] at a dose of 3.0 J/cm^2 or 4.0 J/cm^2. Other HUVECs were subjected to similar treatment with HMME alone or light illumination alone to serve as controls. After light irradiation, fresh medium was added to replace the PBS, the cells were maintained at 37 °C for an additional 24 h before they were analyzed.

2.4. Observation of cell morphological changes

About 2.5 × 10^5 cells were seeded into each well of a 6-well plate. The same treatment was given to HUVECs as described above, with cells without HMME or without light irradiation serving as controls. We assessed the cellular morphology either immediately or at 24 h after light irradiation using an inverted microscope (Olympus, TAKACHIHO SEISAKUSHO, Japan).

2.5. Cell counting kit-8 (CCK-8) assay

A CCK-8 assay (Dojindo Laboratories Japan) was used to assess cell viability. Three of groups of cells i.e. (0, 3.0, and 4.0 J/cm^2) were tested. 100 μL of HUVEC cells (0.8 × 10^4 cells) were maintained in 96-well plates for 24 h before they were treated with HMME-PDT. They were then treated with HMME at different doses (0, 2.5, 5, 7.5, 10, 15, 20 and 25 μg/ml) for 1 h in the dark and then illuminated with a 532-nm LED light at 3.0 J/cm^2 or 4.0 J/cm^2. The non-illuminated group was the dark control. Subsequently, the cells were cultured for 24 h in darkness. This was followed by addition of 10 μl of CCK-8 reagent followed by incubation for one and a half hours at 37 °C. Using the Varioskan Flash multimode reader (Thermo Fisher Scientific) to measure the absorbance at 450 nm. The following equation was applied to calculate the cell viability: Cell viability (%) = [OD (experiment) − OD (blank)]/[OD(control) − OD (blank)] ×100%. The viability of cells subjected to treatment was compared to that of the vehicle-only control cells (100%) to determine the half-maximal inhibitory) (IC_{50})value. The experiment was repeated at least three times.

2.6. Flow cytometry assay

Annexin V-FITC/PI staining kit (BestBio, BB4101, Shanghai, China) was used to detect apoptosis of HUVEC cells after treatment with HMME-PDT. The HUVECs (2.5 × 10^{5}cells per well) were cultured in 6-well plates. 24 h after HMME-PDT treatment, cells were washed using PBS and re-suspended in 400 μl of binding solution and stained with 10 μl of propidium iodide (PI) and 5 μl of AnnexinV-FITC in darkness for 15 min on ice. A NovoCyte Flow Cytometer (ACEA Biosciences, USA) and the NovoExpress software (ACEA Biosciences, USA) were used to analyze the samples. Cells that were Annexin V-FITC+/PI + and those that were Annexin V-FITC+/PI–were considered to be late necrotic/apoptotic and early apoptotic cells, respectively.

2.7. Immunofluorescence

24 h after PDT treatment, HUVEC cells were removed from the culture plates, washed three times by PBS, followed by fixation with 4% paraformaldehyde for 15 min and permeabilization with 0.5% Triton X-100 for 10 min at room temperature, and blocking with 5% BSA for 1 h at 37 °C. Next, the primary antibody (anti-VEGF-A, Abcam, Cambridge Science Park, UK) diluted at 1:50 was added to the cells at 4 °C overnight. The membranes were washed thrice with PBS and then treated with secondary antibodies (Alexa Fluor 488-labeled goat anti-rabbit IgG, Beyotime, Shanghai, China) and then incubated for 30 min. at 37 °C. After a PBS-wash, cells were treated with DAPI (Beyotime, Shanghai, China) for 10 min. at room temperature. The stained cells were added to antifade mounting medium (Beyotime, China). Finally the stained cells were analyzed with confocal laser scanning microscopy (Zeiss, LSM780, Germany).

2.8. Quantifcation of the secreted VEGF-A levels using ELISA

After seeding 2.5 × 10^5 cells in each well of a 6-well plate, they were then treated with PDT. 24 h after treatment cells were harvested. The concentrations of VEGF-A was quantifed using the Human ELISA Kit (Elabsicence, E-EL-H0111c, Wuhan, China) following the protocols given by the manufacturer.

2.9. Western blotting

About 2.5 × 10^5 cells were plated on 6-well plates, after which they were treated with PDT. Thereafter, they were incubated for 24 h before

they were, collected, and washed using ice-cold PBS. This was followed by lysing with RIPA reagent (Beyotime, Shanghai, China), which included phosphatase inhibitors and protease inhibitors for a 30 min duration on ice. The specimens were then centrifuged at 10,000 × *g*, 15 min × 2), to obtain supernatants that were later subjected to BCA Protein Assay Kit (Beyotime, Shanghai, China) to measure the protein concentration.

SDS-PAGE electrophoresis was used to separate the protein samples at the gel concentrations of 8%, 10% or 12% for mTOR, p-mTOR, P70S6, p-P70S6, Akt, p-AKT, Bax, Bcl-2, and GAPDH. The samples were then transferred used the wet transfer method to a PVDF membrane (Millipore, Massachusetts, USA). 5% non-fat milk was used to block the membranes at room temperature for 1 h followed by treatment primary antibodies overnight at 4 °C. The following antibodies were used: anti-mTOR (1:1000, CST, USA), anti-p-mTOR(1:1000, CST, USA), anti-Akt (1:1000, CST, USA), anti-p-Akt (1:1000, CST, USA), anti-Bcl-2 (1:1000, CST, USA), anti-Bax (1:1000, CST, USA), anti-P70S6 (1:500, Santa Cruz, USA), anti-p-P70S6 (1:500, Santa Cruz, USA), and anti-GAPDH (1:10000, Proteintech Grou, Inc, China). The primary antibodies were removed from the membranes by washing three times with TBST solution, before they were probed using secondary anti-mouse antibody or anti-rabbit antibody (1:5000, BOSTER, ab6721; ab131368, Wuhan, China) at room temperature for two hours. The ChemiDoc XRS + imaging system (Bio-Rad Laboratories, USA) was used to analyze the protein blots and band intensities were calculated using ImageLab 4.0 software (Bio-Rad Laboratories, USA), with GAPDH serving as the control protein.

2.10. Quantitative real-time PCR

About 2.5 × 10^5 HUVECs cells were seeded into each well of a 6-well plate and then treated with PDT. The next step involved washing of the cells after 24 h with cold PBS. RNA was then isolated from the cells using Universal RNA Extraction Kit (TaKaRa, Tokyo, Japan). This 1 μg of RNA served as the template for the synthesis of cDNA usign the PrimeScript RT reagent Kit (Takara, Tokyo, Japan). qPCR reaction was prepared in a 25 μl with TB Green Premix Ex TaqII kit (Takara, Tokyo, Japan) and carried out in a CFX-96 Real-Time PCR Detection System (Bio-Rad, Hercules, CA, USA). Table 1 shows the list of all PCR primers used for this experiment. The formula $2^{-\Delta\Delta CT}$ was utilized to calculate the relative mRNA expression of the targeted genes using the BioRadCFX Manager sofware. The expression levels of the genes were normalized to the mRNA levels of GAPDH. As a calibration, a vehicle control group was included to facilitate quantification.

2.11. Statistical analysis

Data are presented as mean ± SD calculated from at least 3 independent tests. All analyses were carried out using one-way ANOVA. $P < 0.05$ was taken to be a statistically significant difference.

Table 1
The primer sequences used in the experiments.

Genes	Primers sequences	
Bax	Forward	5′AGTGGCAGCTGACATGTTTT 3′
	Reverse	5′GGAGGAAGTCCAATGTCCAG 3′
Bcl-2	Forward	5′GCCCTGTGGATGACTGAGTA 3′
	Reverse	5′GGCCGTACAGTTCCACAAAG 3′
GAPDH	Forward	5′CGGAGTCAACGGATTTGGTCGTAT 3′
	Reverse	5′AGCCTTCTCCATGGTGGTGAAGAC 3′

3. Results

3.1. HMME-mediated PDT exerts cytotoxic effects on HUVEC cells

Cell viability was determined by a CCK8 assay to evaluate the effects of different concentrations of HMME-PDT on HUVEC cells. As shown in Fig. 1A, no marked difference in viability was observed between the three groups with different concentrations of HMME (HMME < 25 μg/ml) in the dark (0 J/cm^2) and the cell viability treated was approximately 100% in all cases, indicating that HMME exhibits low dark toxicity at doses less than 25 μg/ml (Fig. 1A). By contrast the viability of HUVECs treated with PDT at a fluence of 3 J/cm^2 or 4 J/cm^2, was significantly reduced. When the light intensity was 3 J/cm^2 or 4 J/cm^2, the viability of cells decreased as the HMME concentration increased. Meanwhile, the viability also decreased as the light intensity increased using the same concentration of HMME. Measured at 24 h after PDT, the IC_{50} values were 9.489 μg/ml and 4.336 μg/ml when the light intensity was 3 J/cm^2 or 4 J/cm^2, respectively. Thus, HMME-mediated PDT exerts cytotoxic effects on HUVEC cells and these results are related both to the light intensity and the photosensitizer concentration.

3.2. Prominent morphological changes showing apoptosis after PDT

To further study HMME-PDT induced cell death, cells were observed under an inverted microscope. We observed significant morphological changes in HUVECs following the HMME-PDT. As shown in Fig. 1B and 1C, the cells treated without HMME or without light irradiation showed adherent growth with clear contours, and no sign of cell apoptosis. In contrast, after PDT treatment with 10 μg/ml Hemoporfin and 3 J/cm^2 or 4 J/cm^2 of light, the cell membrane bubbled, more cells became rounded, shrunken and detached from each other, some floated in the supernatant (Fig. 1D). These are prominent morphological signs of apoptosis.

3.3. HMME-PDT induces apoptosis in HUVEC cells

PDT can lead to cell apoptosis or necrosis [15]. Apoptosis was measured by flow cytometry following Annexin V-FITC/PI staining to determine which cell death pathway was induced by HMME-PDT. As shown in Fig. 2A, flow cytometry results show that non-PDT groups, incubated with Annexin V-FITC and PI, showed that no apoptosis and no necrosis occurred. Meanwhile, after PDT the four groups including viable cells (FITC and PI negative), cells undergoing early apoptosis (FITC positive and PI negative), cells in the late stage of apoptosis (FITC and PI positive) and necrosis (FITC negative and PI positive) could be observed. 24 h after PDT, incubation with 10 μg/ml HMME and irradiation with 3 J/cm^2 or 4 J/cm^2, the apoptotic rate was 60.69% and 81.10% (Fig. 2A). As shown in Fig. 2B, a significant difference was observed between the PDT and non-PDT groups ($P < 0.05$).

To further confirm that the HMME-PDT induced apoptosis of HUVECs, cells were stained with DAPI at 24 h post-treatment with a light intensity of 3 J/cm^2 or 4 J/cm^2 and a concentration of 10 μg/ml HMME. As shown in Fig. 2C, the control cells exhibited homogenous chromatin morphology. After the PDT treatment, the cells exhibited the morphological features of apoptotic cells, such as nuclear condensation with more pronounced DAPI staining, nuclear fragmentation or chromatin condensation, and marginalization (Fig. 2C).

To further probe induction of apoptosis, western blot analyses of apoptosis related proteins and qRT-PCR analyses of mRNAs were performed. Relative to the control group, the protein levels of the experimental PDT group showed light intensity-dependent up-regulation of the pro-apoptotic protein Bax, and down-regulation of the expression of the anti-apoptotic protein Bcl-2 (Fig. 2D). A significant increase in the

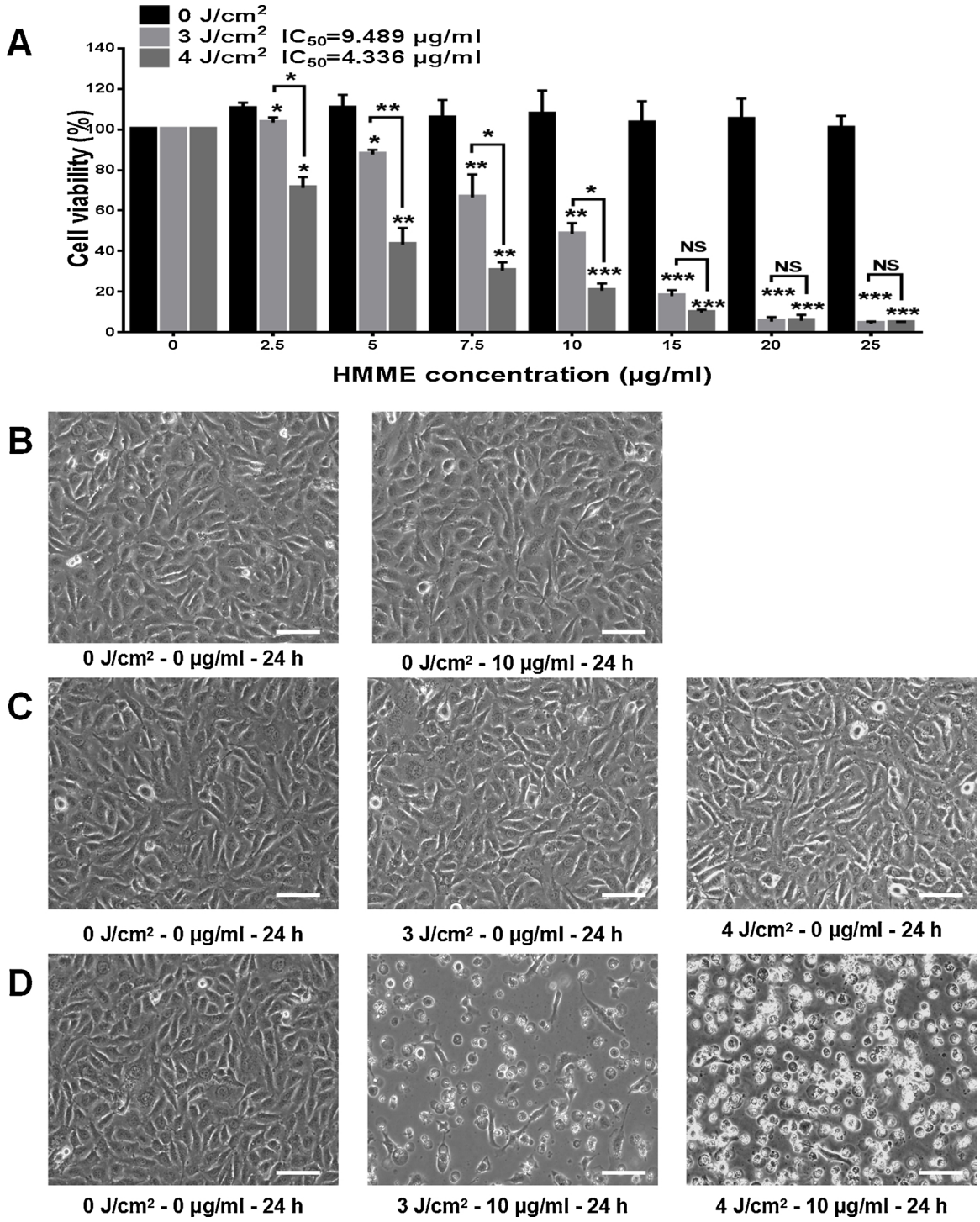

Fig. 1. Inhibition of the growth of HUVECs at 24 h after HMME-PDT.
(A) Cell viability was detected by CCK-8 assay. HUVECs were treated with increasing concentrations of HMME (0–25 μg/mL), and the light intensity was 0 J/cm^2, 3 J/cm^2 or 4 J/cm^2. The viability of the treated cells was compared to the control cells (100%). Data are presented as means ± SD (n = 3); *P < 0.05, **P < 0.01, ***P < 0.001, NS, P > 0.05. (B–C) The effects of HMME-PDT on morphological changes in HUVECs. Bars, 100 μm.

Bax/Bcl-2 protein ratio (Western blot) in the PDT groups was observed comparing the PDT and non-PDT groups (P < 0.05) (Fig. 2E). A similar trend for an increase in the ratio of Bax/Bcl-2 mRNAs (RT qPCR) was observed after PDT (Fig. 2F).

3.4. HMME-PDT blocked the VEGF-A/Akt /mTOR pathway

The role of vascular endothelial growth factors (VEGF) have been shown to be one of the most important regulators of angiogenesis [20]. PDT-treated cells exhibited significantly decreased of VEGF-A at 24 h post-treatment and using the same concentration of HMME the degree of reduction depended on the intensity of the light (Fig. 3A). To further investigate the anti-angiogenic effects of PDT, we measured the protein secretion of VEGF-A using an ELISA Kit. As shown in Fig. 3B, after PDT treatment, the secretion of VEGF-A was decreased significantly, especially in the 4 J/cm^2 light fluence group.

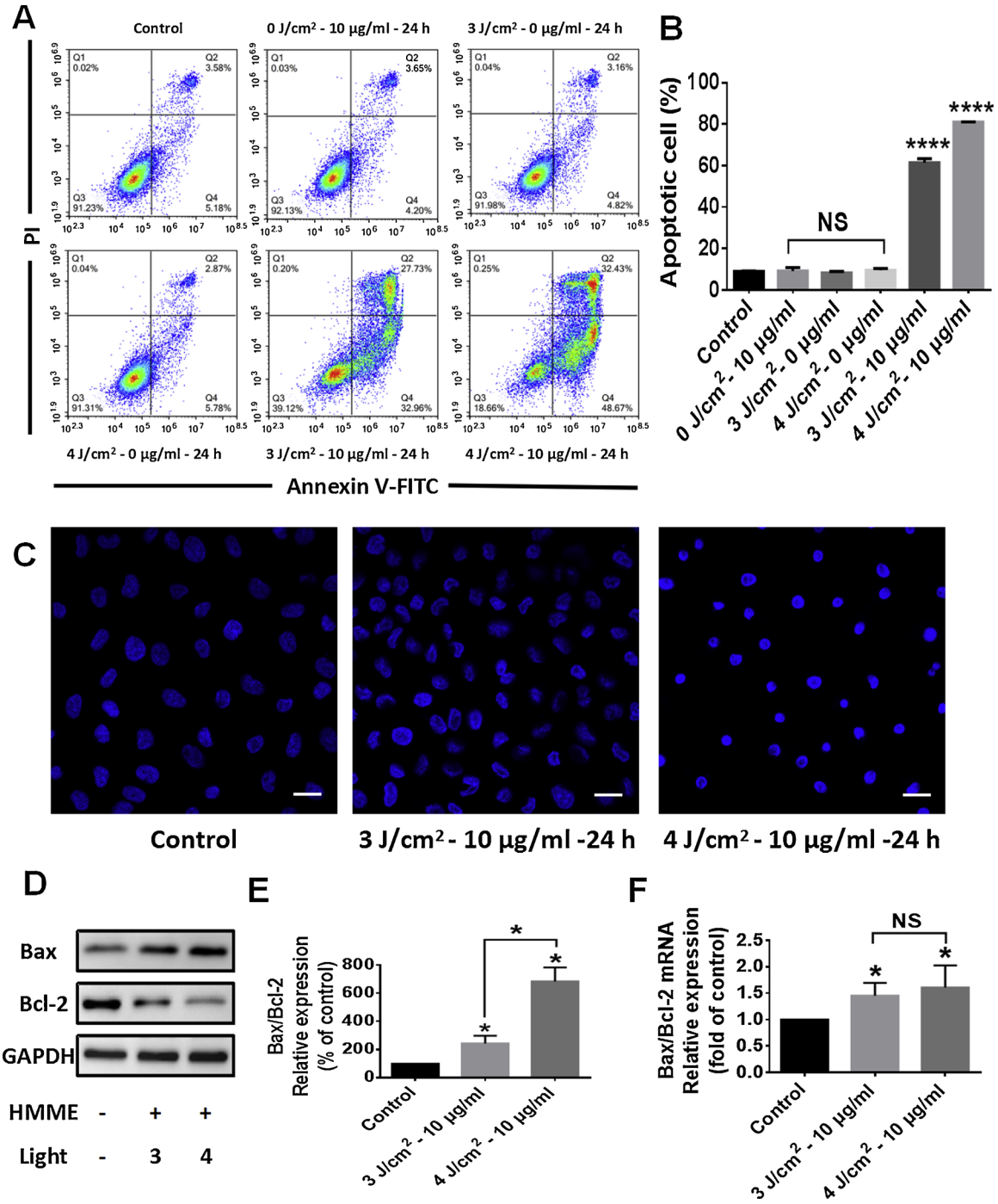

Fig. 2. HMME-PDT induced expression of apoptotic mediators in HUVECs.
(A–B) Flow cytometry analysis of apoptosis in HUVECs treated with HMME-PDT based on Annexin V/PI staining. The bar graphs show the percentage of apoptotic cells for each of the indicated conditions. Data are presented as means ± SD (n = 3), ****P < 0.0001. (C) The HUVECs were stained with DAPI to label the cell nuclei and observed by fluorescence microscopy. Bars, 20 μm. (D–E) Effects of HMME-PDT on protein expression levels of Bax and Bcl-2 were determined by western blot. Quantitative analysis was performed by measuring the relative expression levels of Bax and Bcl-2 to that of GAPDH. Data are expressed as means ± SD,*P < 0.05. (F) The effect of HMME-PDT on Bax and Bcl-2 gene expression. The relative expression mRNAs for Bax and Bcl-2 measured by qRT-PCR using $2^{(-\Delta\Delta Ct)}$ method. The results are expressed as mean ± SD,*p < 0.05.

To investigate whether HMME-PDT can suppress the VEGF/Akt/mTOR pathway, the expression of p-Akt, and total Akt proteins, p-mTOR, and total mTOR proteins, p-P70S6, and total P70S6 proteins were measured. Compared to the control, the expression of the p-Akt, p-mTOR, total mTOR, p-P70S6 and total P70S6 proteins all decreased in a HMME concentration-dependent manner (Fig. 3C). These results suggested that HMME-PDT was capable of suppressing VEGF-A expression, thereby inhibiting Akt, mTOR and P70S6 activation (Fig. 3D). These findings supported the hypothesis that HMME-PDT inhibited the VEGF-A-mediated Akt/mTOR pathway, and suggests alternative mechanisms to inhibit cell growth.

4. Discussion

In the past several decades, the pulsed dye laser (PDL) has been the gold standard treatment for PWS. However, recent data have suggested

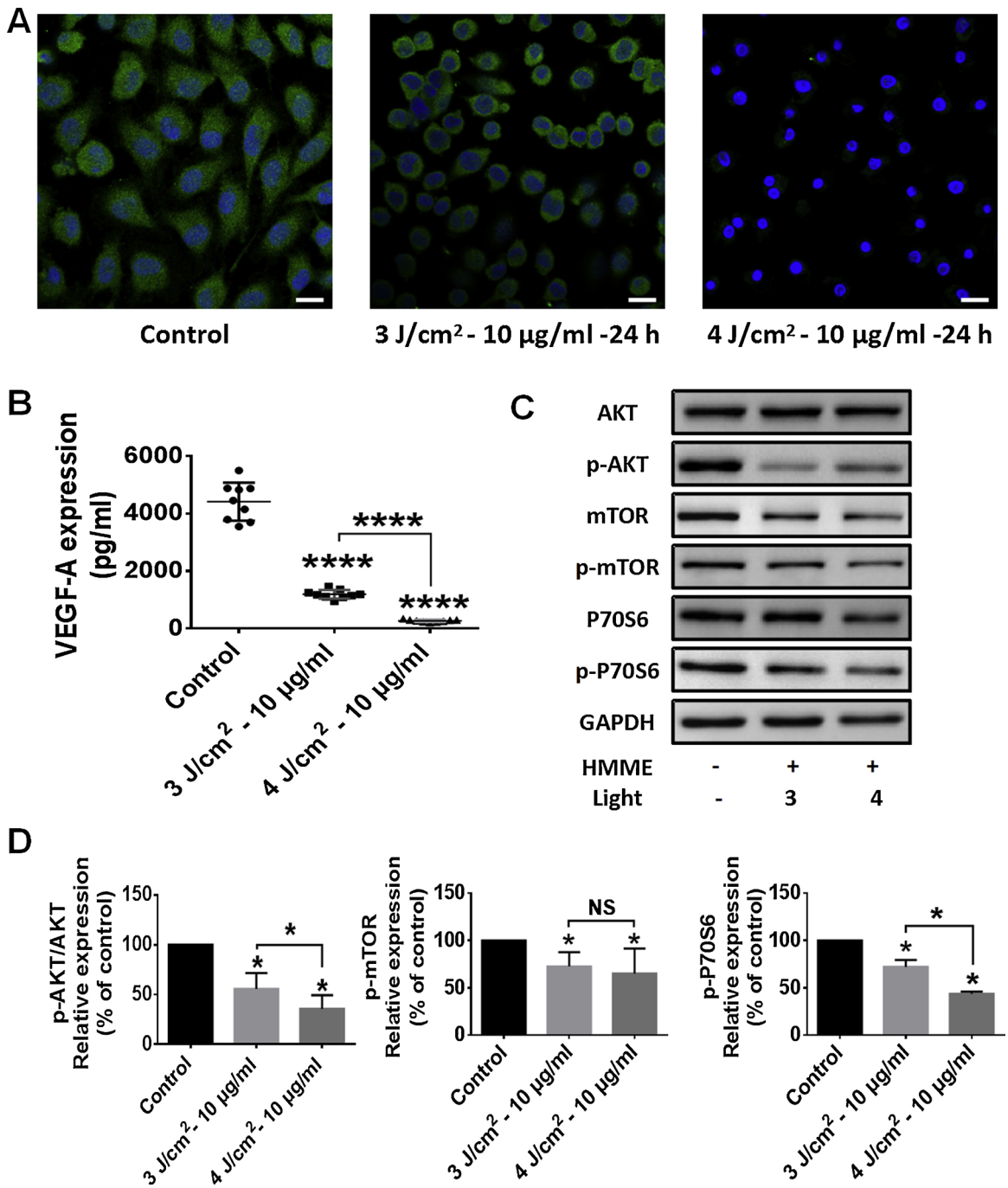

Fig. 3. Inhibition of VEGF-A-mediated VEGFA/Akt /mTOR pathway in HUVECs.
(A) Immunofluorescence analysis of the expression of VEGF-A in HUVECs after HMME-PDT by confocal laser scanning microscope. Bars, 20 μm. (B) The secretion of VEGF-A was measured in the cell culture supernatants by ELISA. Data are presented as means ± SD (n = 9), ****P < 0.0001. (C–D) HMME-PDT affects the protein expression levels of VEGFA/Akt/mTOR signaling molecules in HUVECs. Western blot analysis was used to measure the expression levels of AKT, p-AKT, mTOR, p-mTOR, P70S6, p-P70S6. Quantitative analysis was performed by measuring the relative proteins expression level to that of GAPDH. Data are expressed as means ± SD. *P < 0.05.

that possible revascularization and regeneration of blood vessels post-PDL treatment, is a critical barrier to an adequate therapeutic outcome of PDL treatment for PWS [21]. Although PDL treatment of PWS causes intense, acute damage to blood vessels, at the same time, PDL-induced local hypoxia leads to upregulation of hypoxia-inducible factor-1 alpha (HIF-1α), a master regulator for the hypoxic response [22,23]. When HIF-1α is stabilized and translocated to the nucleus, it results in the transcription of numerous pro-angiogenic genes, including vascular endothelial growth factor (VEGF) [22,23]. VEGF is the predominant growth factor that regulates angiogenesis pathways by signaling via VEGF receptor-2 (VEGFR-2) [24]. Activation of VEGFR-2 will lead to activation of many downstream pathways, including phosphatidylinositol 3-kinases (PI3K), AKT, and the mammalian target of rapamycin (mTOR) signaling [22,25–27], finally resulting in regeneration and revascularization of PWS blood vessels. Therefore, this is the main limitation of traditional PDL treatment for PWS.

In the past decades, published data has recorded that several thousand PWS cases have been treated by PDT, mediated by various

haematoporphyrin-based photosensitizers in China [28–30]. The comparison of side-by-side clinical outcomes from PDL and PDT treatments has demonstrated that PDT is overall more effective in many cases compared to PDL. However, the long half-life of haematoporphyrin derivatives leads to many complications, such as dark toxicity, due to the prolonged skin photosensitivity to sunshine and even strong indoor lighting. Consequently, when patients have been administered haematoporphyrin derivatives, they are required to avoid sun exposure for up to 4 to 12 weeks [30,31]. Poor patient compliance with this requirement has adversely limited their clinical applications [32]. However, it is undeniable that haematoporphyrin derivatives are effective to mediate PDT for vascular malformations. Therefore, it is necessary to find a novel haematoporphyrin derivative for clinical application that lacks side-effects.

The second generation photosensitizer, Hemoporfin (7(12)-(1-methoxyethyl) -12(7)-(1-hydroxyethyl)-3,8,13,17-tetramethyl-21H,23H-porphin-2,18-dipropionic acid) is a novel porphyrin derivative which processes a stable reproducible structure, a high singlet oxygen yield, high photoactivity, low dark toxicity and a fast clearance rate [13]. Recently, clinical outcomes from HMME-PDT treated PWS have shown impressive efficacy. However, the exact mechanisms of action are unclear. In this study, HUVECs were used to explore the phototoxic effects of Hemoporfin. Our results showed that Hemoporfin had a very potent inhibiting effect on HUVECs at very low concentrations. After 24 h of PDT, the HUVECs IC_{50} values were 9.489 μg/ml and 4.336 μg/ml when the light intensity was 3 J/cm^2 or 4 J/cm^2, respectively. Thus, Hemoporfin-mediated PDT exerts cytotoxic effects on HUVEC cells and these results are related to the light intensity and the sensitizer concentration. It is worth noting that in the cell viability studies of HUVECs, Hemoporfin displayed negligible biological activity in the absence of light.

Mammalian cells possess genetically regulated processes that lead to death of cells in a multi-pathway and multi-step manner, which is broadly known as apoptosis [33]. Apoptosis is critical in embryonic development, inhibits the spread of viruses and modulates cell differentiation and development in organisms. Thus, apoptosis is regarded to be an active programmed process of cell death associated with characteristic cytoplasmic and nuclear features [34]. During PDT treatment, the killing of target cells is largely mediated by cellular DNA damage, necrosis and/or apoptosis [35]. In our study, we found obvious signs of apoptosis in the cells at 24 h after PDT with Hemoporfin, suggesting that apoptosis plays a vital role in the therapeutic efficacy of PDT with Hemoporfin. To reinforce this observation, DAPI staining for the nucleus, PI staining and annexin V-FITC techniques were applied to investigate the cell death mode of HUVECs at 24 h after HMME-PDT. In order to reduce damage to the normal tissue, we selected 10 μg/ml HMME and 3 J/cm^2 or 4 J/cm^2 as a light dose. As demonstrated by flow cytometry, apoptosis was observed in HUVECs, and the number of apoptotic cells in the PDT groups was meaningfully higher than non-PDT groups. We also found the level of apoptosis and late apoptosis (necrosis) were elevated with increasing light intensity doses. Nuclear staining showed typical apoptotic bodies, nuclear condensation, nuclear fragmentation or chromatin condensation, marginalization after cells were subjected to PDT with Hemoporfin. These results showed that HMME-PDT promoted both apoptosis and necrosis in HUVECs, and also demonstrated that apoptosis is a crucial form of cell death in the PDT process.

PDT is recognized an effective approach to destroy anti-apoptotic proteins, such as Bcl-2, and also to stimulate proteins that trigger apoptosis [16]. The Bcl-2 family comprises several proteins, some of which are thought to prevent apoptosis while other do the opposite and promote apoptosis [36]. For example, Bcl-2 inhibits apoptosis while Bax stimulates apoptosis [36]. Relative to the control group, HMME-PDT showed light dose-dependent up-regulation of Bax expression, together with a reduction of Bcl-2 expression. A significant difference in Bax/Bcl-2 ratio was observed in protein levels measured by Western blot and also in mRNA expression measured by RT-qPCR. The bax/Bcl-2 ratio determines the functions of the caspase-regulated apoptotic pathway. This is because Bcl-2 may interact with Bax thus sequestering it, and inhibiting the downstream targets of the mitochondrial death cascade [37]. All these findings indicate that HMME-mediated PDT promotes HUVEC cell death via apoptotic pathway.

As a member of the VEGF family, VEGF-A has been implicated in endothelial cell tube formation, and sprouting, and proliferation of endothelial cells [26,27]. VEGF-A functions as a growth factor, which is involved in the angiogenesis process [26]. After activation by VEGF-A, VEGFR-2 triggers a wide range of effects and responses in endothelial cells, including vascular tube formation, endothelial migration and proliferation [24,38]. VEGF-A mediates important survival effects by influencing the PI3K/Akt signaling pathway [39]. PI3K/AKT in turn signals through mTOR, which is one of the kinases targeted by PI3K/AKT, to regulate angiogenesis, survival, growth, and tumor cell proliferation. Interestingly, we found that the protein levels of VEGF-A, p-Akt, p-mTOR, total mTOR, p-P70S6 and total P70S6 were reduced in an HMME concentration-dependent manner. These data imply that HMME-PDT may inhibit VEGF-A expression, suppressing Akt, mTOR and P70S6 activation. The results presented here reveal additional mechanisms through which PDT inhibits vascular endothelial cell growth. It is noteworthy that the PDT process relies on oxygen. During hypoxic stress, cells respond by stimulating angiogenesis by increasing angiogenesis promoting factors, such as VEGF [40]. However, our findings showed that VEGF-A was downregulated at 24 h after PDT treatment. This led to the inhibition of VEGF-A-triggered PI3K/Akt signaling. This observation may account for the low incidence of relapses in PWS following HMME-PDT treatment [41].

In conclusion, our study proved that Hemoporfin-mediated PDT can promote apoptosis and suppress cell growth in HUVECs. The phototoxicity of Hemoporfin was dose-dependent in HUVECs. Taken together, HMME-PDT can also induce apoptosis and inhibit the activation of the VEGF-A-mediated Akt/mTOR pathway.

Disclosure of potential conflicts of interest

Michael R Hamblin discloses the following potential conflicts of interest. Dr Hamblin is on the following Scientific Advisory Boards Transdermal Cap Inc, Cleveland, OH BeWell Global Inc, Wan Chai, Hong Kong Hologenix Inc. Santa Monica, CA LumiThera Inc, Poulsbo, WA Vielight, Toronto, Canada Bright Photomedicine, Sao Paulo, Brazil Quantum Dynamics LLC, Cambridge, MA Global Photon Inc, Bee Cave, TX Medical Coherence, Boston MA NeuroThera, Newark DE JOOVV Inc, Minneapolis-St. Paul MN AIRx Medical, Pleasanton CA FIR Industries, Inc. Ramsey, NJ UVLRx Therapeutics, Oldsmar, FL, Ultralux UV Inc, Lansing MI Illumiheal & Petthera, Shoreline, WA MB Lasertherapy, Houston, TX ARRC LED, San Clemente, CA Varuna Biomedical Corp. Incline Village, NV, Niraxx, Boston, MA. Dr Hamblin has been a consultant for Lexington Int, Boca Raton, FL USHIO Corp, Japan Merck KGaA, Darmstadt, Germany Philips Electronics Nederland B.V. Johnson & Johnson Inc, Philadelphia, PA Sanofi-Aventis Deutschland GmbH, Frankfurt am Main, Germany. Dr Hamblin is a stockholder in Global Photon Inc, Bee Cave, TX, Mitonix, Newark, DE.

None disclosures are for Yingjuan Mei, Xiangling Xiao, Lili Fan, Qichao Liu, Mengxue Zheng, Bing Ni, Rui Yin.

Acknowledgements

This research was supported by the National Natural Science Foundation of China (81571902) and Southwest hospital Incubation project, Third Military Medical University (Army Medical University) (SWH2016LHYS-08) to Rui Yin. Michael R Hamblin was supported by US NIH grants R01AI050875 and R21AI121700.

References

[1] A.H. Jacobs, R.G. Walton, The incidence of birthmarks in the neonate, Pediatrics 58 (2) (1976) 218–222.
[2] M. Malm, M. Carlberg, Port-wine stain–a surgical and psychological problem, Ann. Plast. Surg. 20 (6) (1988) 512–516.
[3] S.H. Barsky, S. Rosen, D.E. Geer, J.M. Noe, The nature and evolution of port wine stains: a computer-assisted study, J. Invest. Dermatol. 74 (3) (1980) 154–157.
[4] J. Wang, Y.Y. Zhu, Z.Y. Wang, X.H. Yao, L.F. Zhang, H. Lv, S.P. Zhang, B. Hu, Analysis of quality of life and influencing factors in 197 Chinese patients with port-wine stains, Medicine (Baltimore) 96 (51) (2017) e9446.
[5] Y. Zhao, J. Tao, P. Tu, Quantitative evaluation of efficacy of photodynamic therapy for port-wine stains using erythema index image analysis, Photodiagnosis Photodyn. Ther. 10 (2) (2013) 96–102.
[6] L.A. Brightman, R.G. Geronemus, K.K. Reddy, Laser treatment of port-wine stains, Clin. Cosmet. Investig. Dermatol. 8 (2015) 27–33.
[7] A. Asahina, T. Watanabe, A. Kishi, N. Hattori, A. Shirai, S. Kagami, R. Watanabe, A. Le Pavoux, T. Maekawa, K. Tamaki, K. Ohara, Evaluation of the treatment of port-wine stains with the 595-nm long pulsed dye laser: a large prospective study in adult Japanese patients, J. Am. Acad. Dermatol. 54 (3) (2006) 487–493.
[8] P. Agostinis, K. Berg, K.A. Cengel, T.H. Foster, A.W. Girotti, S.O. Gollnick, S.M. Hahn, M.R. Hamblin, A. Juzeniene, D. Kessel, M. Korbelik, J. Moan, P. Mroz, D. Nowis, J. Piette, B.C. Wilson, J. Golab, Photodynamic therapy of cancer: an update, CA Cancer J. Clin. 61 (4) (2011) 250–281.
[9] T.J. Dougherty, C.J. Gomer, B.W. Henderson, G. Jori, D. Kessel, M. Korbelik, J. Moan, Q. Peng, Photodynamic therapy, J. Natl. Cancer Inst. 90 (12) (1998) 889–905.
[10] D.E. Dolmans, D. Fukumura, R.K. Jain, Photodynamic therapy for cancer, Nat. Rev. Cancer 3 (5) (2003) 380–387.
[11] A.M. Bugaj, Targeted photodynamic therapy–a promising strategy of tumor treatment, Photochem. Photobiol. Sci. 10 (7) (2011) 1097–1109.
[12] T.C. Lei, G.F. Glazner, M. Duffy, L. Scherrer, S. Pendyala, B. Li, X. Wang, H. Wang, Z. Huang, Optical properties of hematoporphyrin monomethyl ether (HMME), a PDT photosensitizer, Photodiagnosis Photodyn. Ther. 9 (3) (2012) 232–242.
[13] Y. Pu, W. Chen, Z. Yu, Research progress of Hemoporfin–part one: preclinical study, Photodiagnosis Photodyn. Ther. 9 (2) (2012) 180–185.
[14] R.D. Almeida, B.J. Manadas, A.P. Carvalho, C.B. Duarte, Intracellular signaling mechanisms in photodynamic therapy, Biochim. Biophys. Acta 1704 (2) (2004) 59–86.
[15] P. Mroz, A. Yaroslavsky, G.B. Kharkwal, M.R. Hamblin, Cell death pathways in photodynamic therapy of cancer, Cancers (Basel) 3 (2) (2011) 2516–2539.
[16] N.L. Oleinick, R.L. Morris, I. Belichenko, The role of apoptosis in response to photodynamic therapy: what, where, why, and how, Photochem. Photobiol. Sci. 1 (1) (2002) 1–21.
[17] S. Ali, S. Chee, G. Yuen, M. Olivo, Photodynamic therapy induced Fas-mediated apoptosis in human carcinoma cells, Int. J. Mol. Med. (2002) 257–270.
[18] K. Plaetzer, T. Kiesslich, C.B. Oberdanner, B. Krammer, Apoptosis following photodynamic tumor therapy: induction, mechanisms and detection, Curr. Pharm. Des. 11 (9) (2005) 1151–1165.
[19] K.H. Yuan, Z. Huang, Evolving role of PDT in PWS, Photodiagnosis Photodyn. Ther. 4 (3) (2007) 149–150.
[20] M. Kowanetz, N. Ferrara, Vascular endothelial growth factor signaling pathways: therapeutic perspective, Clin. Cancer Res. 12 (17) (2006) 5018–5022.
[21] W. Jia, V. Sun, N. Tran, B. Choi, S.W. Liu, M.C. Mihm Jr., T.L. Phung, J.S. Nelson, Long-term blood vessel removal with combined laser and topical rapamycin anti-angiogenic therapy: implications for effective port wine stain treatment, Lasers Surg. Med. 42 (2) (2010) 105–112.
[22] C. Coulon, M. Georgiadou, C. Roncal, K. De Bock, T. Langenberg, P. Carmeliet, From vessel sprouting to normalization: role of the prolyl hydroxylase domain protein/hypoxia-inducible factor oxygen-sensing machinery, Arterioscler. Thromb. Vasc. Biol. 30 (12) (2010) 2331–2336.
[23] G.H. Fong, Regulation of angiogenesis by oxygen sensing mechanisms, J. Mol. Med. 87 (6) (2009) 549–560.
[24] P. Carmeliet, R.K. Jain, Molecular mechanisms and clinical applications of angiogenesis, Nature 473 (7347) (2011) 298–307.
[25] J. Karar, A. Maity, PI3K/AKT/mTOR pathway in angiogenesis, Front. Mol. Neurosci. 4 (2011) 51.
[26] J.A. Nagy, A.M. Dvorak, H.F. Dvorak, VEGF-A and the induction of pathological angiogenesis, Annu. Rev. Pathol. 2 (2007) 251–275.
[27] N. Ferrara, VEGF-A: a critical regulator of blood vessel growth, Eur. Cytokine Netw. 20 (4) (2009) 158–163.
[28] Z. Huang, Photodynamic therapy in China: over 25 years of unique clinical experience Part two-clinical experience, Photodiagnosis Photodyn. Ther. 3 (2) (2006) 71–84.
[29] Q. Xiao, Q. Li, K.H. Yuan, B. Cheng, Photodynamic therapy of port-wine stains: long-term efficacy and complication in Chinese patients, J. Dermatol. 38 (12) (2011) 1146–1152.
[30] H. Qiu, Y. Gu, Y. Wang, N. Huang, Twenty years of clinical experience with a new modality of vascular-targeted photodynamic therapy for port wine stains, Dermatol. Surg. 37 (11) (2011) 1603–1610.
[31] Z.P. Qin, K.L. Li, L. Ren, X.J. Liu, Photodynamic therapy of port wine stains-a report of 238 cases, Photodiagnosis Photodyn. Ther. 4 (1) (2007) 53–59.
[32] Y. Gu, N.Y. Huang, J. Liang, Y.M. Pan, F.G. Liu, Analyse clinique de 1 949 angiomes plans traités par thérapie photodynamique vasculaire (Gu's PDT), Annales de Dermatologie et de Vénéréologie 134 (3) (2007) 241–244.
[33] C.A. Pettigrew, T.G. Cotter, Deregulation of cell death (apoptosis): implications for tumor development, Discov. Med. 8 (41) (2009) 61–63.
[34] M.C. Jackel, M.A. Dorudian, D. Marx, U. Brinck, A. Schauer, W. Steiner, Spontaneous apoptosis in laryngeal squamous cell carcinoma is independent of bcl-2 and bax protein expression, Cancer 85 (3) (1999) 591–599.
[35] C.A. Robertson, D.H. Evans, H. Abrahamse, Photodynamic therapy (PDT): a short review on cellular mechanisms and cancer research applications for PDT, J. Photochem. Photobiol. B 96 (1) (2009) 1–8.
[36] A. Gross, BCL-2 family proteins as regulators of mitochondria metabolism, Biochim. Biophys. Acta 1857 (8) (2016) 1243–1246.
[37] P.J. Dlugosz, L.P. Billen, M.G. Annis, W. Zhu, Z. Zhang, J. Lin, B. Leber, D.W. Andrews, Bcl-2 changes conformation to inhibit Bax oligomerization, EMBO J. 25 (11) (2006) 2287–2296.
[38] S. Koch, L. Claesson-Welsh, Signal transduction by vascular endothelial growth factor receptors, Cold Spring Harb. Perspect. Med. 2 (7) (2012) a006502.
[39] S. Fulda, Modulation of mitochondrial apoptosis by PI3K inhibitors, Mitochondrion 13 (3) (2013) 195–198.
[40] C.W. Pugh, P.J. Ratcliffe, Regulation of angiogenesis by hypoxia: role of the HIF system, Nat. Med. 9 (6) (2003) 677–684.
[41] K. Gao, Z. Huang, K.H. Yuan, B. Zhang, Z.Q. Hu, Side-by-side comparison of photodynamic therapy and pulsed-dye laser treatment of port-wine stain birthmarks, Br. J. Dermatol. 168 (5) (2013) 1040–1046.